RESEARCH ARTICLE

Special Section:
Climatic and Biotic Events of the Paleogene: Earth Systems and Planetary Boundaries in a Greenhouse World

Key Points:
- A trait-based plankton model is applied to the Eocene in an Earth system model
- Model predictions are broadly consistent with available data on plankton size in the Eocene
- Integration of a trait-based modeling approach with the fossil record is a key future challenge

Supporting Information:
- Supporting Information S1
- Figure S1
- Figure S2
- Figure S3
- Figure S4

Correspondence to:
J. D. Wilson,
jamie.wilson@bristol.ac.uk

Linking Marine Plankton Ecosystems and Climate: A New Modeling Approach to the Warm Early Eocene Climate

J. D. Wilson[1] , F. M. Monteiro[1], D. N. Schmidt[2] , B. A. Ward[1,3], and A. Ridgwell[1,4]

[1]School of Geographical Sciences, University of Bristol, Bristol, UK, [2]Department of Earth Sciences, University of Bristol, Bristol, UK, [3]Ocean and Earth Science, University of Southampton, Southampton, UK, [4]Department of Earth Sciences, University of California, Riverside, CA, USA

Abstract The fossil record reveals large changes in marine plankton ecosystems linked with both environmental and ecological change across the Cenozoic. An understanding of the drivers of these changes is key to understanding the marine carbon cycle. The response of plankton ecosystems in past warm climates also provides a key analogue for current climate change. While models are employed to quantify interactions between the environment and the biota, current Earth system models strongly encode our understanding of modern marine ecosystems. By contrast, trait-based models aim to describe the marine plankton ecosystem in terms of fundamental ecological and physiological rules that are less likely to change through time. This provides a unique opportunity to assess the interactions between marine ecosystem and paleoclimate. For the first time, we apply a size-structured trait-based plankton ecosystem model embedded in the Earth system model of intermediate complexity, cGENIE, to model plankton communities for the warm climate of the early Eocene. Compared to modern, we find the warm climate is associated with an increase in the mean cell size of plankton communities and export production, particularly in the southern high latitudes, along with lower total phytoplankton biomass. Paleogeography has an important role in regulating the effect of ecosystem structure via changes in ocean circulation and nutrient cycling. Warmer temperatures also drive changes due to enhanced zooplankton grazing. An integration of the fossil record with plankton ecosystem models will provide a powerful tool to assess the impacts of warm climates on marine systems.

1. Introduction

Marine plankton communities are an integral component of the marine carbon cycle. By producing and exporting organic carbon and calcium carbonate ($CaCO_3$) from the surface ocean as sinking particles, they play a role in regulating and moderating climate over a range of timescales; by sequestering carbon in the deep ocean and deep-sea sediments (e.g., Hain & Sigman, 2014). Nutrient supply, light levels, and regulation by zooplankton grazing have long been recognized as key first-order controls on marine organic carbon production. However, the biodiversity and community structure of marine plankton ecosystems are being increasingly recognized as also playing a dynamic role in the export and recycling of organic carbon and $CaCO_3$ (e.g., Guidi et al., 2016; Pörtner et al., 2014). The fossil record reveals large changes in marine plankton ecosystems linked with both environmental and ecological changes across the Cenozoic including: the end-Cretaceous extinction event (Henehan et al., 2016) and the associated recovery (Hull, 2015), the Paleocene-Eocene Thermal Maximum (McInerney & Wing, 2011), and long-term changes in response to climate across the Cenozoic (Finkel et al., 2007; Schmidt et al., 2004). Understanding the drivers of these changes, as well as the implications for changes in biogeochemistry and climate, is key to understanding the carbon cycle in the past as well as providing an analogue for current climate change (Schmidt, 2018).

The warm climate of the early Cenozoic provides an ideal starting point to explore the interactions between plankton ecology and climate. A wide range of proxies including oxygen isotopes, Mg/Ca ratios, and biomarkers suggest surface temperatures were warmer, particularly at higher latitudes (Zachos et al., 2008). Our understanding of plankton ecosystems during this time is based on those plankton groups with hard parts preserved in the fossil record, for example, coccolithophores (calcareous nannoplankton), foraminifera, radiolarians, diatoms, and dinoflagellates (primarily as dinocysts). In comparison to plankton in the modern, calcareous nannoplankton in the early Cenozoic were characterized by similar to higher species diversity

(Bown et al., 2004) and overall larger cell sizes (Hannisdal et al., 2012; Henderiks & Pagani, 2008; Herrmann & Thierstein, 2012). Similar trends are also observed for dinoflagellates (Finkel et al., 2007). In comparison, low-latitude planktonic foraminifera were characterized by smaller sizes in comparison to modern species with diversities slightly higher than today (Norris, 1991). High-latitude species have remained similar sizes on average throughout the Cenozoic (Schmidt et al., 2004).

The size trends in early Cenozoic plankton fossil groups have largely been attributed to environmental factors and long-term variation in climate. A reduced surface to deep ocean gradient of $\delta^{18}O$ during the early Eocene compared to modern, indicating reduced vertical stratification, may have been associated with increased nutrient availability in the surface ocean (Finkel et al., 2007; Schmidt et al., 2004). Higher levels of atmospheric CO_2 would have supported groups without a carbon concentrating mechanism. Additionally, there is evidence that the biogeochemical cycling of nutrients may have been different such as indicated by larger vertical gradients in $\delta^{13}C$, suggesting a more efficient biological pump driven by increased nutrient availability (Hilting et al., 2008). Larger but shallower vertical ocean gradients in $\delta^{13}C$ have also been interpreted as evidence for shallower and more intense remineralization of sinking organic matter due to an increase in metabolic rates of bacteria with warmer temperatures (John et al., 2013, 2014). This would have led to more rapid nutrient cycling in the upper ocean. Lastly, higher temperatures via increased metabolic rates could have additionally influenced ecological interactions such as increased growth rates and zooplankton grazing rates (e.g., Boscolo-Galazzo et al., 2018; Winder & Sommer, 2012).

Numerical models are a useful quantitative tool for testing and understanding the links between plankton biodiversity, biogeochemistry, and climate. A key requirement for applying these models to past warm climates is that the underlying assumptions encoded in the model are valid for past plankton communities. Earth system models of Intermediate Complexity (EMICs) are commonly applied to past climates such as the Eocene with two main approaches to modeling plankton and their effect on biogeochemistry (e.g., Hülse et al., 2017). One approach converts available nutrients/light directly into organic matter and does not resolve plankton biomass (e.g., Ridgwell & Schmidt, 2010). While these models can capture the basic dynamics of nutrient, temperature and light limitations on production, this is parameterized as a function of modern light and temperature fields to match modern observations. As such these models cannot explicitly represent the dynamics associated with resource competition and trophic interactions. EMICs also use Nutrient Plankton Zooplankton Detritus models and plankton functional type models that resolve plankton biomass for a number of different types (e.g., phytoplankton, zooplankton, calcifiers, and silicifers) and their associated dynamics (e.g., Heinze & Ilyina, 2015). However, the representation of plankton in these models are often based on laboratory cultured species experiments (Le Quéré et al., 2005). They typically include the representation of diatoms, which while being important in the modern ocean, rapidly expanded as a group to achieve similar functionality and abundance after the Eocene-Oligocene boundary (Hendry et al., 2018). As such, these models may not be directly applicable to past climates.

"Trait-based" models provide an alternative approach to modeling plankton communities that is not based on prescribing characteristics to individual groups (e.g., Follows et al., 2007; Litchman et al., 2007). Instead, a large number of plankton types are used, each with a set of traits such as maximum growth rate or nutrient affinity, sampled from a range of predefined trade-offs. Plankton communities then emerge from competition for resources and grazing pressure driven by the assigned traits and trade-offs. Here we focus on plankton cell-size, which can be related to multiple traits and trade-offs by well-known allometric relationships (Finkel et al., 2010; Ward et al., 2012). The use of plankton cell size has the particular advantage that size is a measurable quantity of major plankton groups in the fossil record (Finkel et al., 2007; Schmidt et al., 2006; Young, 1990) thereby facilitating potential model-data comparison for past climates. Additionally, size can be related to biogeochemical-relevant processes such as particle sinking rates, which are a factor in both the magnitude of export production (Henson et al., 2011) and nutrient recycling by setting the depth at which sinking particles of organic matter are remineralized (Cram et al., 2018).

In this paper, we take a first step to linking marine plankton ecosystems and climate by applying a new size-structured trait-based plankton model to simulations of the warm background climate of the early Eocene in the Earth system model cGENIE. We explore key features of the modeled plankton communities that can be related to quantities measurable in the fossil record such as plankton size and abundance, as well as quantities that can be related to export production. We test the sensitivity of these results to paleogeography,

the impact of warming on ocean circulation as well as directly on plankton ecology. Finally, we identify key challenges and directions for future research on this theme.

2. Methods

2.1. The cGENIE Earth System Model

We employ the carbon-centric version of the GENIE Earth system model of intermediate complexity: cGENIE. This model has been used successfully to explore the interactions between marine biogeochemistry and climate for a range of timescales and time periods including the Eocene and the PETM (e.g., Gibbs et al., 2015; Gutjahr et al., 2017; John et al., 2014; Norris et al., 2013; Ridgwell & Schmidt, 2010).

The physical model of cGENIE consists of a three-dimensional non-eddy resolving frictional geostrophic ocean circulation model, coupled to a two-dimensional energy-moisture balance model of the atmosphere and a dynamic-thermodynamic sea-ice model (Edwards & Marsh, 2005). The biogeochemistry model represents the transformations and redistribution of essential biogeochemical compounds and isotopes via biological processes (Ridgwell et al., 2007). The biogeochemical model used in previous studies directly converts nutrients into organic matter via an uptake rate that saturates with increasing nutrient concentrations based on Michaelis-Menten kinetics (e.g., Franks, 2002). Organic matter is then partitioned into dissolved organic carbon (DOC), which degrades with a fixed lifetime representing semilabile DOC, and particulate organic carbon (POC). The remineralization of sinking POC with depth is predicted by a globally uniform fixed exponential function. Model parameters are calibrated using modern global annual mean observations. The modern configuration is capable of reproducing the large-scale distribution of nutrients (Ridgwell et al., 2007), carbonate chemistry (Holden et al., 2013), and projected anthropogenic CO_2 inventories consistent with data and model-based reconstructions (Cao et al., 2009).

2.2. Size-Structured Ecological Model: EcoGEnIE

The standard biogeochemical model in cGENIE has an implicit representation of the formation of organic matter by plankton, that is, nutrients are converted directly to organic matter based on nutrient and light availability. Here this is replaced with a newly developed ecological model, "EcoGEnIE", that explicitly resolves the plankton community (Ward et al., 2018; Figure 1). Organic matter production is similarly limited by nutrient availability and light, but now as an explicit plankton biomass pool that is subject to processes such as resource competition and grazing by zooplankton before being passed to DOC and POC. We briefly describe the relevant components of EcoGEnIE here and refer readers to Ward et al. (2018) for further details on its development within cGENIE and to Ward et al. (2012) for details on the initial development of the size-structured model.

EcoGEnIE resolves a number of plankton populations, defined by functional group (phytoplankton and zooplankton) and organism size (equivalent spherical diameter). Each population is associated with biomass state variables for carbon, phosphorus, and chlorophyll (Figure 1). The uptake of nutrients by phytoplankton is governed by a Michaelis-Menten-like function (e.g., Franks, 2002), where maximum uptake rate and nutrient affinity are dependent on the size of the plankton (Figure 1). Smaller phytoplankton have a higher nutrient affinity than larger cells. Carbon is assimilated during photosynthesis using similar size relationships but with a reduction in photosynthetic rates for the smallest cell sizes implicitly reflecting that the demand for nitrogen is high relative to uptake together with a lower efficiency of converting nitrogen into biomass (Marañón et al., 2012; Figure 1). Phytoplankton growth is also subject to an Arrhenius-like dependence on temperature.

Zooplankton grazing is dependent on the concentration of available prey biomass, with a size-dependent maximum grazing rate. The availability of prey biomass is determined as a log-normal function of zooplankton-to-phytoplankton size ratios, with zooplankton predominantly grazing on prey that are 10 times smaller than themselves (in terms of equivalent spherical diameter) because these are less likely to escape and are easier to ingest (Kiørbe, 2008; Figure 1). The production of organic matter is a function of the mortality of all plankton (linearly related to biomass) and the inefficient assimilation of biomass by zooplankton grazing (at least 30% is lost to organic matter as messy feeding and increases as internal quotas of nutrients increase). The export of organic matter as dissolved or particulate forms is also size dependent with the fraction of DOC produced decreasing from 80% to 40% from the smallest to largest cell sizes (e.g., Roshan & DeVries, 2017). Plankton mortality is reduced at very low biomasses such that plankton cannot become extinct ("everything is everywhere"). The model is initialized with homogeneous biomass with size-structured communities emerging as a function of the underlying allometric relationships (Ward et al., 2018; Figure 1).
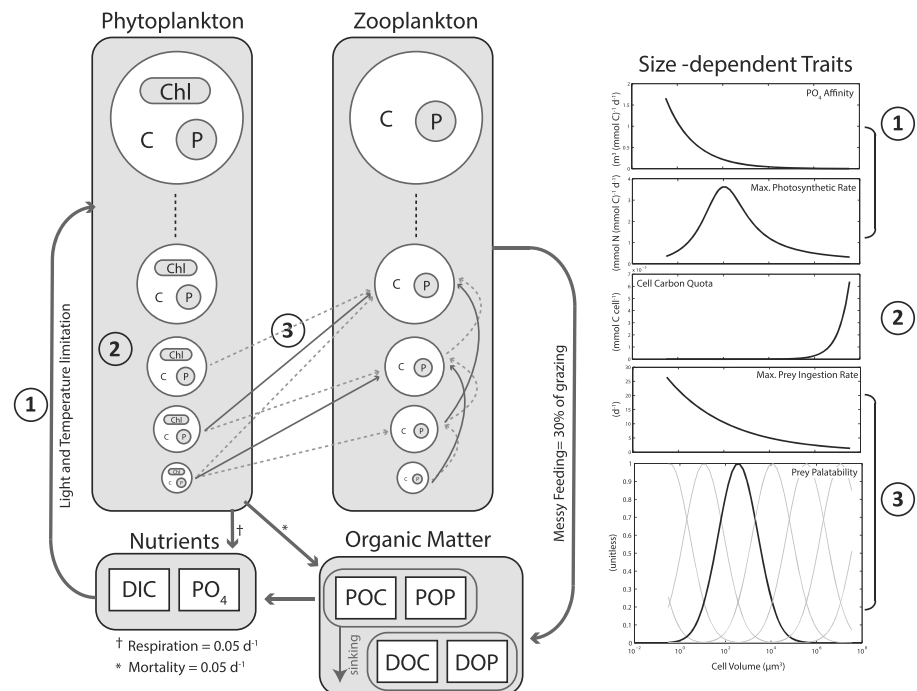
Figure 1. Schematic representation of the size-structured ecological model, "EcoGEnIE" (Ward et al., 2018), showing the key allometric relationships for (1) nutrient affinity and carbon uptake rate, (2) the size of the cell quota for carbon, and (3) zooplankton grazing. The prey palatability panel demonstrates the size preference of prey for an example grazer in black with preferences of zooplankton of other sizes shown in gray. Key fixed parameters are shown where appropriate.

2.3. Experiments

We run the model with late Paleocene early Eocene boundary conditions from Ridgwell and Schmidt (2010), which specifically includes a late Paleocene early Eocene paleogeography (see Figure 2b); atmospheric CO_2 concentration of 834 ppm (3× preindustrial CO_2 of 278 ppm); 0.46% reduced solar constant; seasonally varying wind fields and a globally uniform $CaCO_3$:POC export ratio of 0.2. The inventory of PO_4 is set to the modern inventory. The ecological model has eight phytoplankton and eight zooplankton of sizes 0.6, 1.9, 6.0, 19.0, 60.0, 190.0, 600.0, and 1,900.0 μm (e.g., two picoplankton, two nanoplankton, two microplankton, and two mesoplankton size classes per functional group). The parameters for the ecological model are those set in Ward et al. (2018). The model is run without deep-sea sediments.

We perform a series of experiments to explore the model prediction of plankton communities in the Eocene:

1. Modern—the model is run with preindustrial boundary conditions. The model setup is that of Ward et al. (2018) except there is no iron limitation to allow direct comparison with the Eocene runs.
2. Early Eocene paleogeography—the model is run with late Paleocene early Eocene boundary conditions but with a preindsutrial atmospheric CO_2 concentration of 278 ppm.
3. Early Eocene CO_2 and climate—as experiment 2 but with an atmospheric CO_2 concentration of 834 ppm.
4. Temperature effects on circulation and ecology—the direct effects of warmer temperatures on ecology and those from a changing ocean circulation are separated out. For effects on circulation only, experiment 3 is repeated but with the ecosystem model forced with sea surface temperatures (SSTs) from experiment 2. For effects on ecology only, experiment 2 is repeated but with the ecosystem model forced with SSTs from experiment 3.

All model experiments are spun-up to steady state for 10,000 years from initial conditions. Experiments 2, 3, and 4 are also repeated with modern boundary conditions for comparison and are shown in the supporting information. To illustrate the emergent structure of the model plankton community in an equilibrated ocean environment, we choose a set of model outputs that are specifically relevant to quantities in the fossil and proxy records: mean size (defined as the biomass-weighted geometric mean) of phytoplankton communities (e.g., Finkel et al., 2007), total carbon biomass, and productivity (e.g., Ma et al., 2014). For productivity we show the export production of POC, rather than primary productivity, because it has a key link to nutrient cycling
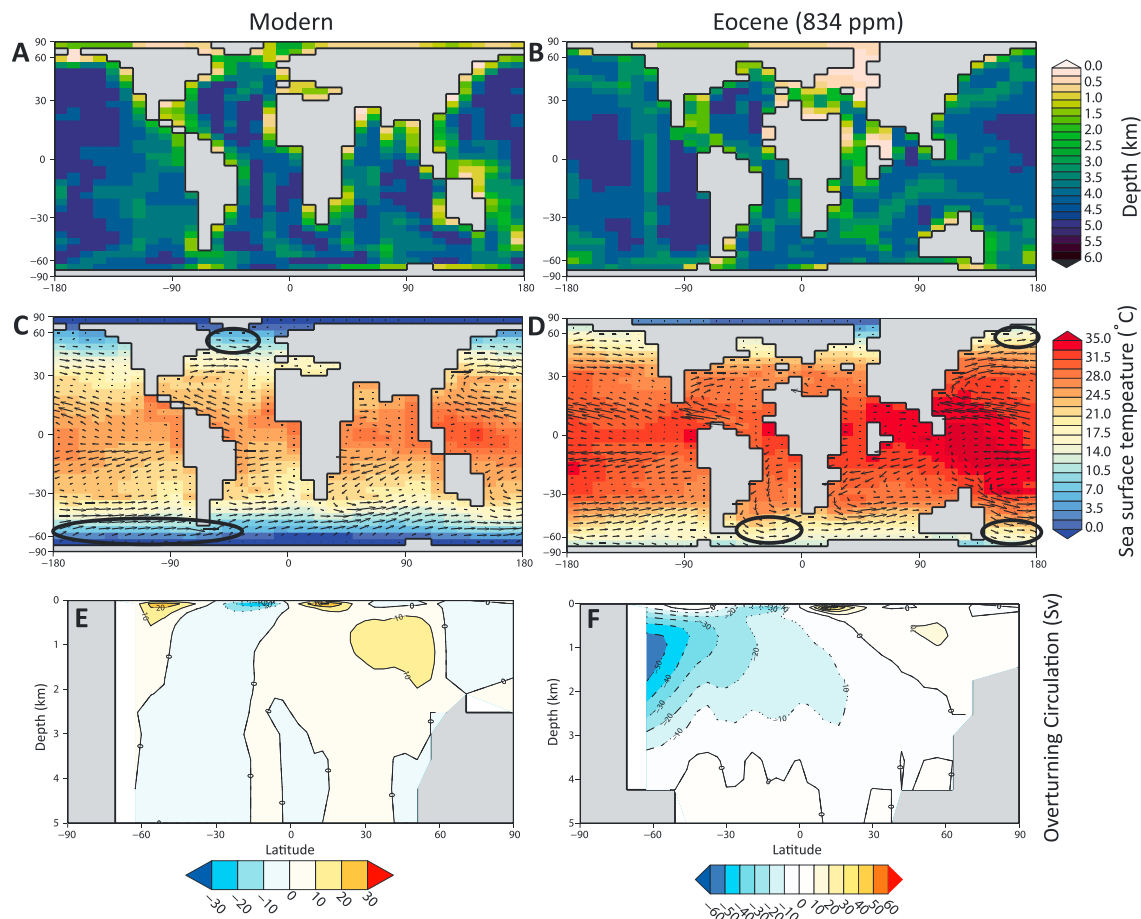
Figure 2. Key environmental parameters for the Eocene and Modern experiments. Parameters shown are the depth of the water column (m; top panels (a) and (b)), sea surface temperatures (°C; middle panels (c) and (d)), and global overturning circulation (Sv; bottom panels (e) and (f)). Overlain on panels (c) and (d) are the patterns of surface ocean circulation. Black circles in panels (c) and (d) indicate areas of deep-water formation.

and biogeochemistry in the ocean interior. We note that these model outputs are not necessarily directly comparable due to the incompleteness of the fossil record and uncertainty surrounding paleoproductivity proxies (Averyt & Paytan, 2004). As such, we focus on broad-scale changes only, that is, basin-scale and latitudinal differences. The challenges of integrating model outputs and data are discussed in section 4.1.

3. Results

The modern run shows features that are consistent with modern observations and other modeling studies. At steady state, smaller phytoplankton with higher nutrient affinities are able to outcompete larger cell sizes for limiting nutrients. Plankton communities in regions such as the subtropical gyres, where nutrient fluxes are low, are dominated by small phytoplankton (<2 μm) and associated with low total phytoplankton biomass and export production (Figure 3a). With increasing nutrient fluxes, an increase in the biomass of smaller phytoplankton is limited by zooplankton grazing such that larger size classes become competitive (Ward et al., 2014). Regions with high nutrient fluxes, such as upwelling zones and subpolar regions, are therefore characterized by the coexistence of size classes, shown here as larger mean sizes (Figure 3a) and higher diversity (Figure S1). These regions are also characterized by higher biomass and export production due to the higher nutrient fluxes. In summary, the total biomass of phytoplankton is controlled by nutrient supply ("bottom-up control") and the biomass of individual size classes and coexistence of size classes is a function of zooplankton grazing ("top-down control"; Ward et al., 2014). Note the preindustrial results here are run without iron limitation but show consistent broad-scale features when run with iron limitation (Figure S4).
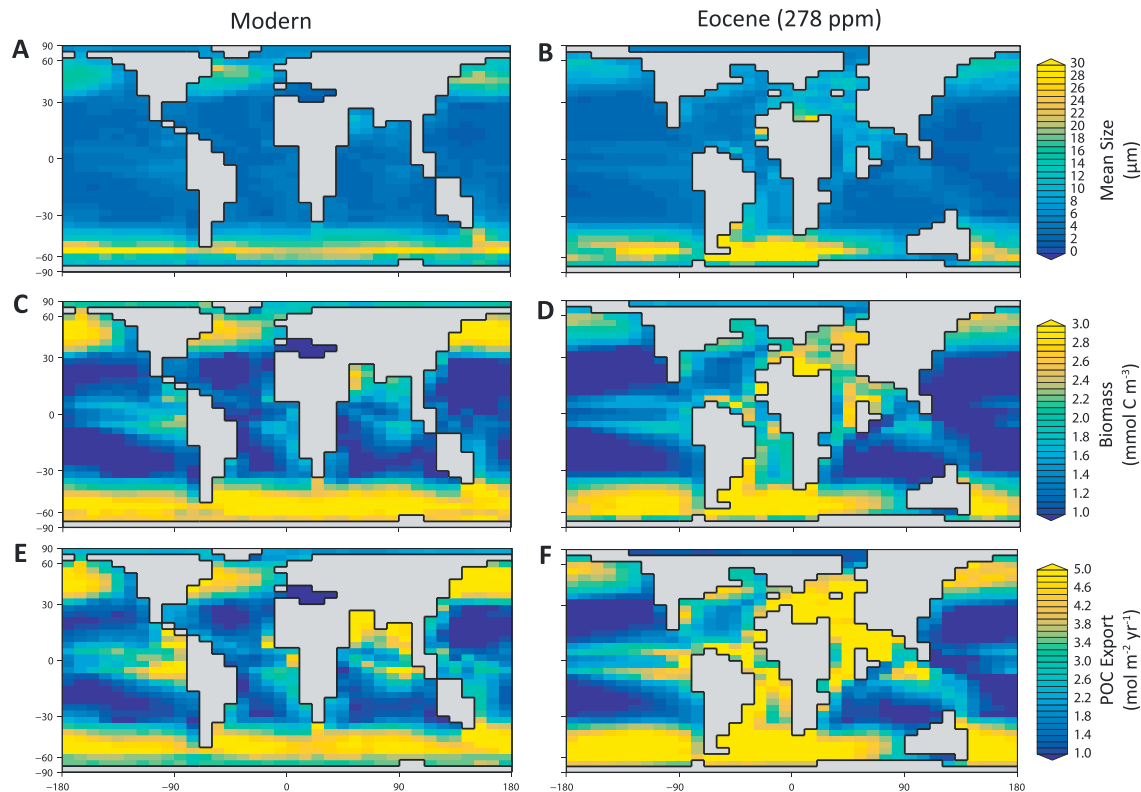
Figure 3. Model predictions of plankton communities for the Eocene paleogeography compared with Modern experiment. From top to bottom, panels (a) and (b) show the biomass-weighted geometric mean size of the phytoplankton community (μm), panels (c) and (d) show the total biomass of phytoplankton (mmol C m^{-3}), and panels (e) and (f) show the export production of particulate organic carbon (mol m^{-2} year^{-1}).

3.1. Role of Eocene Paleogeography

The late Paleocene early Eocene paleogeography differs considerably from the modern configuration with a smaller North Atlantic basin, open circum-tropical seaways, a shallow Tethys Ocean basin, and a constricted Southern Ocean (Figure 2b). The Eocene boundary conditions are also associated with an atmospheric CO_2 concentration of 834 ppm and SSTs that are globally 4 °C higher, with the greatest warming in the high latitudes, compared to the modern run (Figure 2d). The Eocene configuration has a more vigorous ocean circulation with increased global overturning at steady state (minimum of −57 Sv and maximum of 45 Sv) than the modern configuration (minimum of −37 Sv and maximum of 39 Sv; Figure 2f). We first separate the effects of Eocene paleogeography and a warmer climate by running the Eocene run with preindustrial CO_2 concentrations of 278 ppm. The global overturning circulation for the Eocene paleogeography is relatively similar (minimum of −51 Sv and maximum of 46 Sv) to the full Eocene run but with SSTs that are closer to the preindustrial run (not shown).

The modeled plankton communities for the early Eocene paleogeography differ predominantly in the Southern high latitudes (Figures 3 and 4) where the region of larger mean cell size occurs over a broader range of latitudes than in the predindustrial run (Figure 4a). Maximum zonal average mean size of communities increases by 5 μm with larger increases locally (Figure 4a). This size increase is also associated with concurrent increases in biomass and export production (Figures 3d and 3f). In contrast, the open ocean low-latitude communities, excluding the Tethys, are similar to the modern communities except for slightly lower biomass and productivity in the subtropical gyres (Figures 3 and 4). The Tethys Ocean has a unique geometry with a shallow and relatively enclosed basin (Figure 2b). Along with the southern Atlantic, the model predicts that these regions are more similar to the modern Arabian Sea and upwelling regions of the southern Atlantic than regions at similar latitudes. In particular, the southern Atlantic lacks a distinct open ocean gyre (Figure 3). Overall, latitudinal patterns of size diversity are similar between the modern and Eocene paleogeography (Figure S1).
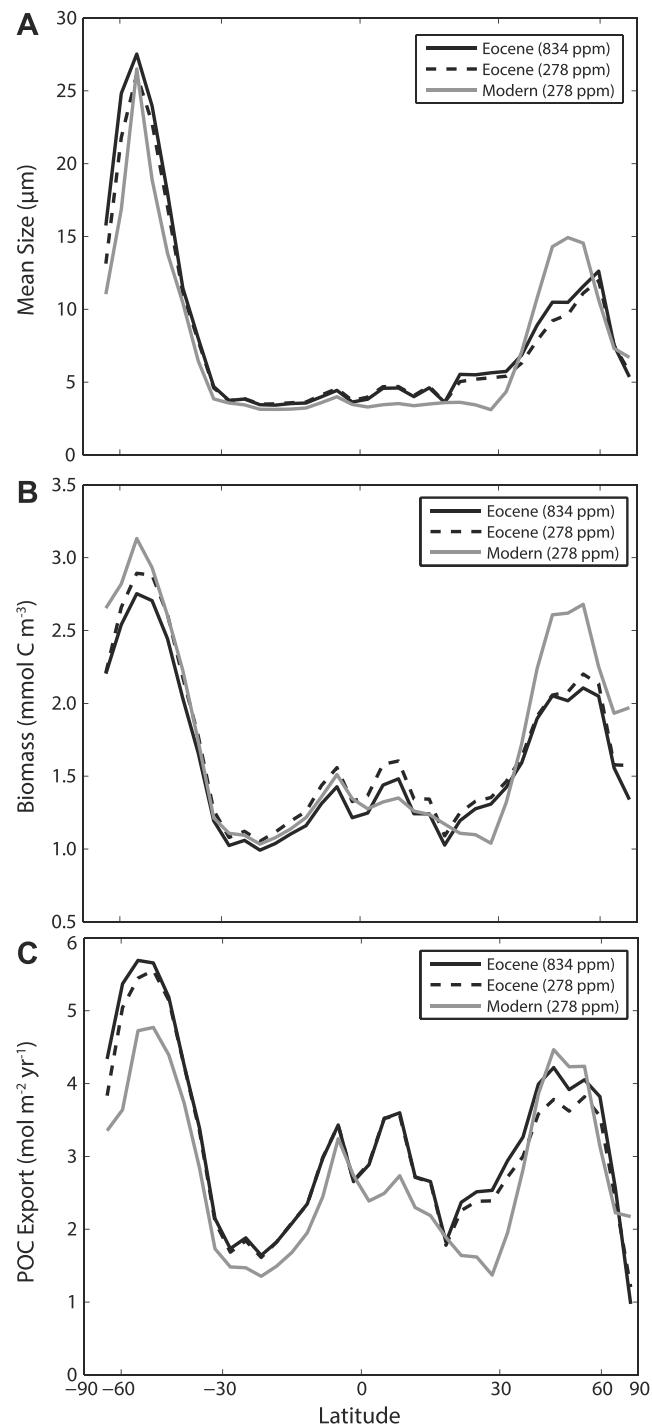
Figure 4. Zonal averages of (a) biomass-weighted geometric mean size of phytoplankton (μm), (b) total phytoplankton biomass (mmol C m^{-3}), and (c) export production of particulate organic carbon (mol m^{-2} year^{-1}). The full-black line shows the results from the full Eocene experiment, and the black dashed line shows the Eocene paleogeography experiment. The gray line shows the results from the Modern experiment.
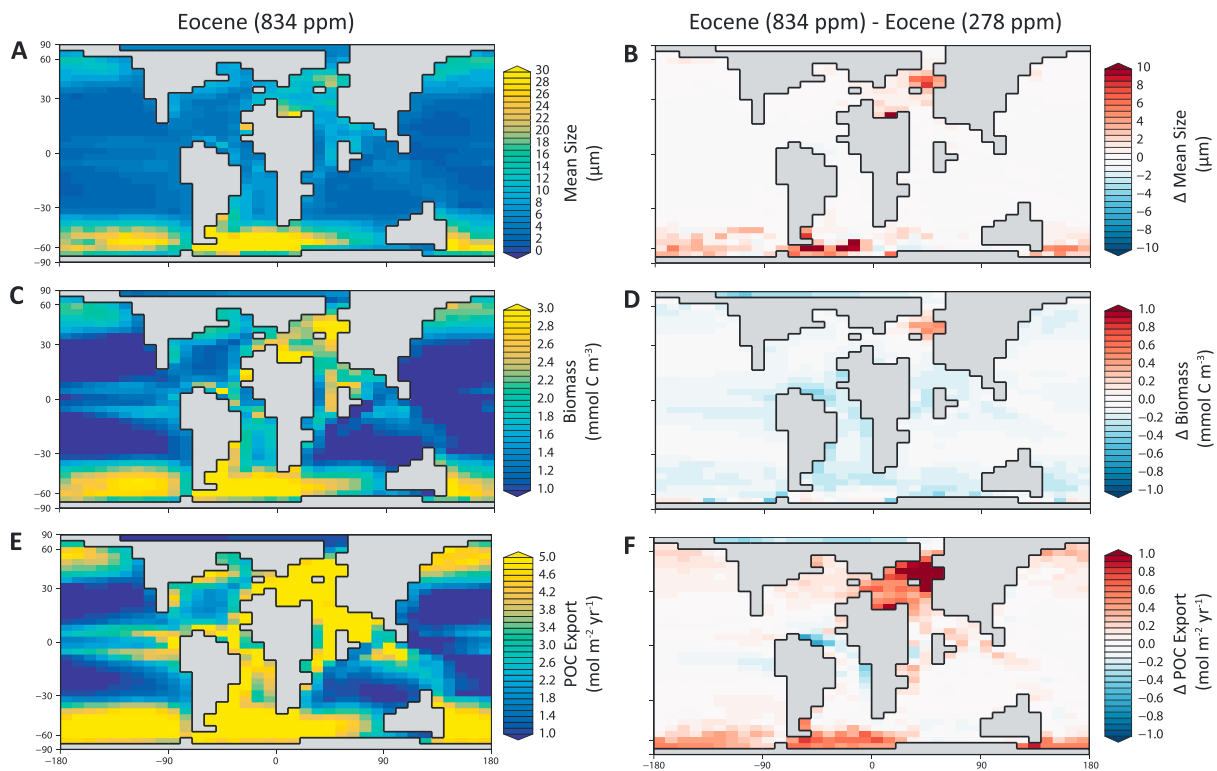
Figure 5. Model predictions of plankton communities for the full Eocene experiment compared with the paleogeography only experiment. Panel (a) shows the biomass-weighted geometric mean size of the phytoplankton community (μm), panel (c) shows the total biomass of phytoplankton (mmol C m^{-3}), and panel (e) shows the export production of particulate organic carbon (mol m^{-2} year^{-1}). Panels (b), (d), and (f) show the differences between panels (a), (c), and (e) and the modern run.

The increase in mean cell size, biomass, and POC export in the Southern high latitudes is driven by increased nutrient fluxes associated with a more vigorous ocean circulation as shown by the stronger overturning circulation compared with modern (Figures 2e and 2f). A higher nutrient flux delivered to the surface ocean is able to support the coexistence of larger plankton size classes, thereby increasing the mean size of plankton communities. Additionally, the largest plankton cell sizes are located in regions of deep-water formation where vertical mixing and nutrient fluxes are strongest (Figures 3b and 2d). In comparison, the relatively restricted and shallow Tethys basin is likely to be associated with the relatively intense local nutrient recycling, supporting the larger plankton cell sizes in this region.

3.2. Role of Eocene CO$_2$ and Climate

To explore the effect of CO$_2$ and climate we run the model with the full Eocene configuration of paleogeography and an atmospheric CO$_2$ concentration of 834 ppm (Figure 5). The warmer climate acts to accentuate the features observed with the Eocene paleogeography. The high latitudes (>35°N and 40°S), particularly the Southern Ocean, experience an increase in mean cell sizes by up to 10 μm (associated with the coexistence of larger phytoplankton size classes alongside the pre-existing size structure; Figure 4a). These regions are also associated with increasing POC export. Low latitudes (<20° from the equator) are relatively unchanged (Figures 5 and 4). A feature that is nonintuitive is a global decrease in plankton biomass with increasingly warm climates (Figure 5d).

These features described above result in part from the ecological model in response to a warmer climate, for example, temperature-dependent growth and grazing rates, but also from physical changes such as the supply of nutrients to the surface ocean driven by a changing ocean circulation. To isolate the changes driven by a changing ocean circulation the full Eocene run was repeated but with the ecological model forced with SSTs from the paleogeography run, that is, the plankton communities experience SSTs associated with an atmospheric CO$_2$ concentration of 278 ppm. Differences between the SST-forced experiments and the Eocene paleogeography experiment show that physical changes only drive significant changes in the plankton communities of the Tethys Ocean (Figures 6a, 6c, and 6e). The strength of the ocean circulation in cGENIE has a
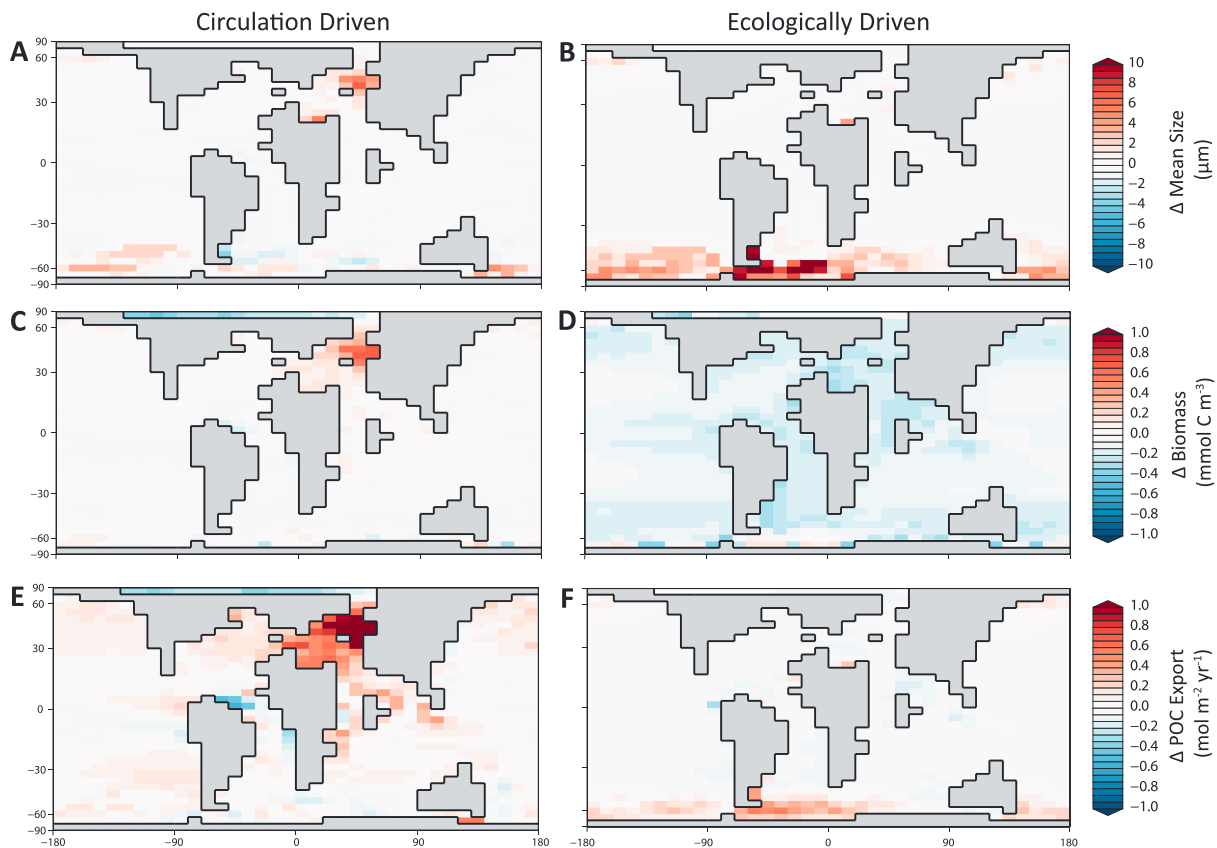
Figure 6. Effects of temperature changes on plankton ecosystems separated by effects on ocean circulation (left panels) and effects directly on plankton physiology (right panels). Panels (a), (c), and (e) correspond to an atmospheric CO_2 concentration of 834 ppm but with plankton communities separately forced with SSTs from the paleogeography experiment at 278 ppm. Panels (b), (d), and (f) correspond to an atmospheric CO_2 concentration of 278 ppm but with plankton communities separately forced with SSTs from the paleogeography experiment at 834 ppm. All panels show the difference between the SST-forced experiment and the paleogeography experiment.

relatively low sensitivity to increasing atmospheric CO_2 (e.g., Monteiro et al., 2012) as demonstrated by the small change in global overturning between the full Eocene experiment and the paleogeography experiment (ranges of −57 to 45 and −51 to 46 Sv, respectively).

To isolate the physiological effect of warmer temperatures on plankton communities, the Eocene paleogeography experiment is repeated but with plankton communities separately forced with SSTs from the full Eocene experiment, that is, plankton communities experience SSTs associated with 834 ppm but nutrient fluxes associated with 278 ppm. The SST forced experiment is compared with the paleogeography experiment (Figures 6b, 6d, and 6f). With the exception of the Tethys, the majority of global changes associated with plankton communities and a warmer climate are driven by temperature-dependent processes in the ecological model. In EcoGEnIE, both the uptake of nutrients and the grazing rate of zooplankton are temperature dependent. Despite increasing rates of nutrient and carbon uptake by phytoplankton, there is a drop in phytoplankton biomass globally (Figure 6d) as phytoplankton biomass is increasingly assimilated into zooplankton biomass. As the assimilation of phytoplankton biomass by zooplankton is inefficient (sloppy/messy feeding has a maximum efficiency of 70%; Ward et al., 2018), the increase in zooplankton grazing is associated with an increase in POC export in these regions (Figure 6f). Because zooplankton grazing is a top-down control on the biomass in each size class (Ward et al., 2014), the increased grazing pressure leads to more nutrients being available for larger phytoplankton. This increases the mean cell size of communities, primarily in the high latitudes where nutrient fluxes are higher. In low-nutrient regimes, however, phytoplankton already utilizes upwelled nutrients efficiently such that larger cell sizes cannot be supported.

4. Discussion

We have presented a set of results from a new size-structured ecosystem model that is coupled with an Earth system model and applied to early Eocene boundary conditions. Applying this model to the warm greenhouse climate of the early Eocene is a first step in using plankton models to understand drivers of past changes in plankton communities and the implications for biogeochemistry. In the model a change to early Eocene boundary conditions, including paleogeography and albedo, results in changes in ocean circulation that increases the delivery of nutrients to the surface ocean (bottom-up control). Additionally, we see a direct effect of warmer SSTs, associated with higher atmospheric CO_2, driving changes in plankton communities directly via the temperature dependence of zooplankton grazing (top-down control). At a global level, the increase in mean cell size is broadly consistent with trends in fossil record observations of mean cell size in the early Cenozoic (Finkel et al., 2007). These trends also occur primarily in the high latitudes, with comparatively little change in the low-latitude oceans, which the fossil record is not able to resolve. Our intention here is not to resolve the potential drivers behind the trend in mean cell size across the Cenozoic. Instead, we discuss the processes in our model that create these features as a precursor to future studies.

Our results highlight that one key requirement for modeling past ecosystems is the fidelity of the predicted ocean circulation, as this is a key constraint on nutrient fluxes to the surface ocean. Our model predicts higher overturning increases the rate of nutrient cycling globally, consistent with an interpretation that reduced vertical stratification through the Cenozoic has driven the long-term decrease in mean cell sizes (Finkel et al., 2007; Schmidt et al., 2004). Despite the coarse resolution and parameterized physics of cGENIE, the model has agreement with a late Paleocene composite of benthic foraminiferal δ^{13}C, suggesting a reasonable simulation of deep-water formation locations and large-scale circulation patterns (Kirtland Turner & Ridgwell, 2013). Additionally, the vertical temperature profiles are similar to those in higher-resolution ocean models of the Eocene (e.g., John et al., 2014). The meridional overturning structure in cGENIE (Figure 2f) is also similar in structure to higher-resolution models (Lunt et al., 2010; Heinze & Ilyina, 2015) although is notably stronger, potentially leading to an overestimation of surface nutrient fluxes.

Fluxes of nutrients to the surface ocean are additionally sensitive to the recycling of particulate organic matter in the water column. Changes in the depth of remineralization, driven by changes in either sinking velocity and/or remineralization rates, can alter the distribution of nutrients in the ocean (Kwon et al., 2009). For example, warmer temperatures during the early Cenozoic may have increased the rate of microbial activity, leading to more rapid nutrient cycling higher up in the water column (Boscolo-Galazzo et al., 2018). Other potentially significant mechanisms include size-dependent sinking velocities, ballasting of organic matter by minerals, aggregation dynamics, fast sinking zooplankton pellets, and fragmentation of sinking particles by zooplankton (e.g., Hülse et al., 2017). The significance of these mechanisms in the modern ocean is still highly uncertain, but many are related to plankton community structure (e.g., Cram et al., 2018; Guidi et al., 2016).

Our results demonstrate the importance of trophic interactions in driving global changes in cell size and ecosystem characteristics due to the temperature dependence of zooplankton grazing. These results are largely consistent with a number of mesocosm and model experiments that predict a loss of phytoplankton biomass with increased grazing pressure under warmer temperatures and an associated shift in food web structure (Chen et al., 2012; O'Connor et al., 2009; Olonscheck et al., 2013). An increase in mean cell size is also consistent with outputs from an ecosystem model that explored the response of plankton communities to anthropogenic climate change in the 21st century (Lefort et al., 2015). Heterotrophy is expected to be up to 2 times more sensitive to temperature changes than photosynthesis (Boscolo-Galazzo et al., 2018), whereas these are treated uniformly in EcoGEnIE. As such, the effect of increased grazing pressure here is likely an underestimate.

There are factors not considered in this study that may also contribute to changes in ecosystem composition in the early Cenozoic: the global inventory of phosphate and fluxes of iron. The global inventory of phosphate in these experiments is maintained at the modern inventory as changes in the phosphate are currently not well constrained (Föllmi, 1995). However, an increase in phosphate globally would lead to relatively greater nutrient availability and an increase in cell sizes, biomass, and POC export. Note the phosphate inventory in these experiments is fixed by assuming all organic phosphorus reaching the seafloor is remineralized and so does not include any feedbacks from changes in organic carbon burial and weathering. Second, our experiments omit an iron cycle as the magnitude and source of iron fluxes is likely to have been different in the early Cenozoic (Horner et al., 2015). Running our modern experiments with an iron cycle

(e.g., Ward et al., 2018) results in decreases in mean cell size, biomass, and POC export in the high latitudes that are of similar magnitude to changes observed in our experiments (Figure S4). This is very dependent on the spatial pattern of atmospheric deposition, which is likely to vary with changing climatic conditions, as well as atmospheric deposition being the most important source of iron (e.g., Horner et al., 2015).

4.1. Linking the Fossil Record, Marine Ecosystems, and Climate

A challenge for integrating model results with fossil records is the incomplete nature of the fossil record. Our model represents ecosystems as a whole, whereas large parts of these plankton ecosystems are not preserved in the fossil record, for example, cyanobacteria, large eukaryotes, and other zooplankton groups such as copepods. The key advantage of using a size-based ecosystem model is that cell size is a quantifiable metric in the fossil record. Cell size in our model can potentially correspond with fossil groups, for example, calcifying nannoplankton broadly corresponds with the modeled nanoplankton groups (2–20 μm). Approaches that look at the composition of assemblages may help bridge this gap by moving toward the community-level representation of ecosystem models. For example, Gibbs et al. (2018) derive frequency distributions for the cell size and biomass of nannoplankton communities across the Paleo-Eocene Thermal Maximum. Relating these to indicators of nutrient availability could help distinguish between bottom-up and top-down controls.

A trait-based modeling approach aimed at past climates can be specifically expanded and tested for those groups that leave a fossil record. Our ecological model does not include a representation of the functional types of plankton often considered in biogeochemical modeling such as calcifiers and silicifers (e.g., Le Quéré et al., 2005). This currently limits the application of the model to inform questions about feedbacks over longer timescales, such the role of changes in the $CaCO_3$ flux driving changes in ocean sediment composition (e.g., Hannisdal et al., 2012; Hull, 2015). There is still lots of uncertainty about the sensitivity of calcifiers to processes such as ocean acidification (e.g., Pörtner et al., 2014) making the representation of these plankton, and in particular of calcification, in models potentially difficult. Currently, the production of $CaCO_3$ in both EcoGEnIE and cGENIE is modeled with a rain-ratio approach, commonly used by Earth system models (Hülse et al., 2017). Some progress on representing coccolithophores and the traits and trade-offs in trait-based models has been made (Monteiro et al., 2016). Integrating these into EcoGEnIE would facilitate the evaluation of longer-term feedbacks. Different strategies of plankton, such as mixotrophy, may also be relevant when considering the response of plankton to environmental change. For example, a representation of mixotroph dinoflagellates may be relevant to modeling the PETM, which is characterized by the large increase in the dinoflagellate taxon *Apectodinium* (Sluijs et al., 2007). Mixotrophy has also been applied in trait-based models (Ward & Follows, 2016), which have been used to help explain the radiation of major plankton groups (Knoll & Follows, 2016).

5. Conclusions

Trait-based models of plankton ecosystems, being based on underlying ecological and physiological rules, offer the opportunity to explore the interactions between plankton ecosystems, biogeochemistry, and climate in an Earth system dramatically different from today's. Here we use a new Earth system model that accounts for a size-structured trait-based plankton communities to predict the state of the plankton ecosystems of the warm Eocene climate as a first step in applying this type of model to past climates. We find that marine ecosystems of the warm early Eocene are characterized by larger plankton on average and higher export production than in the modern ocean, with these trends focused in the high latitudes and the Tethys Ocean. These features are primarily associated with the Eocene paleography, which affects the ocean circulation along with warmer temperature driving changes in trophic interactions. Our results are broadly consistent with available records of plankton groups, but further work is needed to generate information about the latitudinal variations and to understand the relationship between fossil plankton groups and the wider ecosystem represented by the model.

References

Averyt, K. B., & Paytan, A. (2004). A comparison of multiple proxies for export production in the equatorial Pacific. *Paleoceanography*, *19*, PA4003. Retrieved from https://agupubs.onlinelibrary.wiley.com/doi/abs/10.1029/2004PA001005, https://doi.org/10.1029/2004PA001005

Boscolo-Galazzo, F., Crichton, K., Barker, S., & Pearson, P. (2018). Temperature dependency of metabolic rates in the upper ocean: A positive feedback to global climate change? *Global and Planetary Change*, *170*, 201–212. Retrieved from http://www.sciencedirect.com/science/article/pii/S0921818118301905, https://doi.org/10.1016/j.gloplacha.2018.08.017

Bown, P. R., Lees, J. A., & Young, J. R. (2004). Calcareous nannoplankton evolution and diversity through time, *Coccolithophores: From molecular processes to global impact*. Berlin, Heidelberg: Springer Berlin Heidelberg, pp. 481–508. https://doi.org/10.1007/978-3-662-06278-4_18

Cao, L., Eby, M., Ridgwell, A., Caldeira, K., Archer, D., Ishida, A., & Yool, A. (2009). The role of ocean transport in the uptake of anthropogenic CO_2. *Biogeosciences*, *6*(3), 375–390. Retrieved from http://www.biogeosciences.net/6/375/2009/

Chen, B., Landry, M. R., Huang, B., & Liu, H. (2012). Does warming enhance the effect of microzooplankton grazing on marine phytoplankton in the ocean? *Limnology and Oceanography*, *57*(2), 519–526. Retrieved from https://aslopubs.onlinelibrary.wiley.com/doi/abs/10.4319/lo.2012.57.2.0519, https://doi.org/10.4319/lo.2012.57.2.0519

Cram, J. A., Weber, T., Leung, S. W., McDonnell, A. M. P., Liang, J. H., & Deutsch, C. (2018). The role of particle size, ballast, temperature, and oxygen in the sinking flux to the deep sea. *Global Biogeochemical Cycles*, *32*(5), 858–876. Retrieved from https://agupubs.onlinelibrary.wiley.com/doi/abs/10.1029/2017GB005710, https://doi.org/10.1029/2017GB005710

Edwards, N., & Marsh, R. (2005). Uncertainties due to transport-parameter sensitivity in an efficient 3-D ocean-climate model. *Climate Dynamics*, *24*(4), 415–433.

Finkel, Z. V., Beardall, J., Flynn, K. J., Quigg, A., Rees, T. A. V., & Raven, J. A. (2010). Phytoplankton in a changing world: Cell size and elemental stoichiometry. *Journal of Plankton Research*, *32*(1), 119–137. Retrieved from https://doi.org.10.1093/plankt/fbp098, https://doi.org/10.1093/plankt/fbp098

Finkel, Z. V., Sebbo, J., Feist-Burkhardt, S., Irwin, A. J., Katz, M. E., Schofield, O. M. E., & Falkowski, P. G. (2007). A universal driver of macroevolutionary change in the size of marine phytoplankton over the Cenozoic. *Proceedings of the National Academy of Sciences*, *104*(51), 20,416–20,420. Retrieved from http://www.pnas.org/content/104/51/20416.abstract, https://doi.org/10.1073/pnas.0709381104

Föllmi, K. B. (1995). 160 m.y. record of marine sedimentary phosphorus burial: Coupling of climate and continental weathering under greenhouse and icehouse conditions. *Geology*, *23*(6), 503. Retrieved from https://doi.org/10.1130/0091-7613(1995)023<0503:MYROMS>2.3.CO;2, https://doi.org/10.1130/0091-7613(1995)023<0503:MYROMS>2.3.CO;2

Follows, M. J., Dutkiewicz, S., Grant, S., & Chisholm, S. W. (2007). Emergent biogeography of microbial communities in a model ocean. *Science*, *315*(5820), 1843–1846. Retrieved from http://www.sciencemag.org/content/315/5820/1843.abstract, https://doi.org/10.1126/science.1138544

Franks, P. J. S. (2002). NPZ models of plankton dynamics: Their construction, coupling to physics, and application. *Journal of Oceanography*, *58*(2), 379–387. Retrieved from https://doi.org/10.1023/A:1015874028196, https://doi.org/10.1023/A:1015874028196

Gibbs, S. J., Bown, P. R., Ridgwell, A., Young, J. R., Poulton, A. J., & O'Dea, S. A. (2015). Ocean warming, not acidification, controlled coccolithophore response during past greenhouse climate change. *Geology*, *44*(1), 59–62. https://doi.org/10.1130/G37273.1

Gibbs, S. J., Sheward, R. M., Bown, P. R., Poulton, A. J., & Alvarez, S. A. (2018). Warm plankton soup and red herrings: Calcareous nannoplankton cellular communities and the Palaeocene-Thermal Maximum. *Philosophical Transactions of the Royal Society of London A: Mathematical, Physical and Engineering Sciences*, *376*, 2130. Retrieved fromhttp://rsta.royalsocietypublishing.org/content/376/2130/20170075,https://doi.org/10.1098/rsta.2017.0075

Guidi, L., Chaffron, S., Bittner, L., Eveillard, D., Larhlimi, A., Roux, S., & Gorsky, G. (2016). Plankton networks driving carbon export in the oligotrophic ocean. *Nature*, *532*, 465–470. https://doi.org/10.1038/nature16942

Gutjahr, M., Ridgwell, A., Sexton, P. F., Anagnostou, E., Pearson, P. N., Pälike, H., & Foster, G. L. (2017). Very large release of mostly volcanic carbon during the Palaeo-Eocene Thermal Maximum. *Nature*, *548*, 573–577. https://doi.org/10.1038/nature23646

Hain, M. P., & Sigman, D. M. (2014). *The biological pump in the past* (pp. 485–517). Amsterdam, NL: Elsevier.

Hannisdal, B., Henderiks, J., & Liow, L. H. (2012). Long-term evolutionary and ecological responses of calcifying phytoplankton to changes in atmospheric CO_2. *Global Change Biology*, *18*(12), 3504–3516. Retrieved fromhttps://doi.org/10.1111/gcb.12007, https://doi.org/10.1111/gcb.12007

Heinze, M., & Ilyina, T. (2015). Ocean biogeochemistry in the warm climate of the late Paleocene. *Climate of the Past*, *11*(1), 63–79. Retrieved fromhttp://www.clim-past.net/11/63/2015/, https://doi.org/10.5194/cp-11-63-2015

Henderiks, J., & Pagani, M. (2008). Coccolithophore cell size and the Paleogene decline in atmospheric CO_2. *Earth and Planetary Science Letters*, *269*(3), 576–584. Retrieved from http://www.sciencedirect.com/science/article/pii/S0012821$x08001775,https://doi.org/10.1016/j.epsl.2008.03.016

Hendry, K. R., Marron, A. O., Vincent, F., Conley, D. J., Gehlen, M., Ibarbalz, F. M., & Bowler, C. (2018). Competition between Silicifiers and non-silicifiers in the past and present ocean and its evolutionary impacts. *Frontiers in Marine Science*, *5*, 22. Retrieved from https://www.frontiersin.org/article/10.3389/fmars.2018.00022 , https://doi.org/10.3389/fmars.2018.00022

Henehan, M. J., Hull, P. M., Penman, D. E., Rae, J. W. B., & Schmidt, D. N. (2016). Biogeochemical significance of pelagic ecosystem function: An end-Cretaceous case study. *Philosophical Transactions of the Royal Society of London B: Biological Sciences*, *371*, 1694. Retrieved from http://rstb.royalsocietypublishing.org/content/371/1694/20150510 , https://doi.org/10.1098/rstb.2015.0510

Henson, S. A., Sanders, R., Madsen, E., Morris, P. J., Le Moigne, F., & Quartly, G. D. (2011). A reduced estimate of the strength of the ocean's biological carbon pump. *Geophysical Research Letters*, *38*, L04606. Retrieved from https://doi.org/10.1029/2011GL046735 , https://doi.org/10.1029/2011GL046735

Herrmann, S., & Thierstein, H. R. (2012). Cenozoic coccolith size changes—Evolutionary and/or ecological controls? *Palaeogeography, Palaeoclimatology, Palaeoecology*, *333-334*, 92–106. Retrieved from http://www.sciencedirect.com/science/article/pii/S0031018212001514 ,https://doi.org/10.1016/j.palaeo.2012.03.011

Hilting, A. K., Kump, L. R., & Bralower, T. J. (2008). Variations in the oceanic vertical carbon isotope gradient and their implications for the Paleocene-Eocene biological pump. *Paleoceanography*, *23*, PA3222. Retrieved from https://doi.org/10.1029/2007PA001458

Holden, P. B., Edwards, N. R., Müller, S. A., Oliver, K. I. C., Death, R. M., & Ridgwell, A. (2013). Controls on the spatial distribution of oceanic $\delta^{13}C_{DIC}$. *Biogeosciences*, *10*(3), 1815–1833. Retrieved from http://www.biogeosciences.net/10/1815/2013/, https://doi.org/10.5194/bg-10-1815-2013

Horner, T. J., Williams, H. M., Hein, J. R., Saito, M. A., Burton, K. W., Halliday, A. N., & Nielsen, S. G. (2015). Persistence of deeply sourced iron in the Pacific Ocean. *Proceedings of the National Academy of Sciences*, *112*(5), 1292–1297. Retrieved from http://www.pnas.org/content/112/5/1292, https://doi.org/10.1073/pnas.1420188112

Hull, P. (2015). Life in the aftermath of mass extinctions. *Current Biology*, *25*, R941–R952. https://doi.org/10.1016/j.cub.2015.08.053

Hülse, D., Arndt, S., Wilson, J. D., Munhoven, G., & Ridgwell, A. (2017). Understanding the causes and consequences of past marine carbon cycling variability through models. *Earth-Science Reviews*, *171*, 349–382. Retrieved from http://www.sciencedirect.com/science/article/pii/S0012825216303191, https://doi.org/10.1016/j.earscirev.2017.06.004

John, E., Pearson, P. N., Coxall, H. K., Birch, H., Wade, B. S., & Foster, G. L. (2013). Warm ocean processes and carbon cycling in the Eocene. *Philosophical Transactions of the Royal Society of London A: Mathematical, Physical and Engineering Sciences*, *371*, 2001. https://doi.org/10.1098/rsta.2013.0099

John, E., Wilson, J., Pearson, P., & Ridgwell, A. (2014). Temperature-dependent remineralization and carbon cycling in the warm Eocene oceans. *Palaeogeography, Palaeoclimatology, Palaeoecology*, *413*, 158–166. Retried from http://www.sciencedirect.com/science/article/pii/S0031018214002685, https://doi.org/10.1016/j.palaeo.2014.05.019

Kiørbe, T. (2008). *A mechanistic approach to plankton ecology*. Princeton: Princeton University Press.

Kirtland Turner, S., & Ridgwell, A. (2013). Recovering the true size of an Eocene hyperthermal from the marine sedimentary record. *Paleoceanography*, *28*, 700–712. Retrieved from https://agupubs.onlinelibrary.wiley.com/doi/abs/10.1002/2013PA002541, https://doi.org/10.1002/2013PA002541

Knoll, A. H., & Follows, M. J. (2016). A bottom-up perspective on ecosystem change in Mesozoic oceans. *Proceedings of the Royal Society of London B: Biological Sciences*, *283*, 1841. Retrieved from http://rspb.royalsocietypublishing.org/content/283/1841/20161755, https://doi.org/10.1098/rspb.2016.1755

Kwon, E. Y., Primeau, F., & Sarmiento, J. L. (2009). The impact of remineralization depth on the air-sea carbon balance. *Nature Geoscience*, *2*(9), 630–635. https://doi.org/10.1038/ngeo612

Le Quéré, C., Harrison, S. P., Colin Prentice, I., Buitenhuis, E. T., Aumont, O., Bopp, L., & Wolf-Gladrow, D. (2005). Ecosystem dynamics based on plankton functional types for global ocean biogeochemistry models. *Global Change Biology*, *11*(11), 2016–2040. Retrieved from https://doi.org/10.1111/j.1365-2486.2005.1004.x

Lefort, S., Aumont, O., Bopp, L., Arsouze, T., Gehlen, M., & Maury, O. (2015). Spatial and body-size dependent response of marine pelagic communities to projected global climate change. *Global Change Biology*, *21*(1), 154–164. Retrieved from https://doi.org/10.1111/gcb.12679

Litchman, E., Klausmeier, C. A., Schofield, O. M., & Falkowski, P. G. (2007). The role of functional traits and trade-offs in structuring phytoplankton communities: scaling from cellular to ecosystem level. *Ecology Letters*, *10*(12), 1170–1181. Retrieved from https://doi.org/10.1111/j.1461-0248.2007.01117.x

Lunt, D. J., Valdes, P. J., Jones, T. D., Ridgwell, A., Haywood, A. M., Schmidt, D. N., & Maslin, M. (2010). CO_2-driven ocean circulation changes as an amplifier of Paleocene-Eocene thermal maximum hydrate destabilization. *Geology*, *38*(10), 875–878. Retrieved from https://doi.org/10.1130/G31184.1, https://doi.org/10.1130/G31184.1

Ma, Z., Gray, E., Thomas, E., Murphy, B., Zachos, J., & Paytan, A. (2014). Carbon sequestration during the Palaeocene-Eocene Thermal Maximum by an efficient biological pump. *Nature Geoscience*, *7*, 382–388. https://doi.org/https://doi.org/10.1038/ngeo2139

Marañón, E., Cermeõ, P., López-Sandoval, D. C., Rodríguez-Ramos, T., Sobrino, C., Huete-Ortega, M., & Rodrguez, J. (2012). Unimodal size scaling of phytoplankton growth and the size dependence of nutrient uptake and use. *Ecology Letters*, *16*(3), 371–379. Retrieved from https://onlinelibrary.wiley.com/doi/abs/10.1111/ele.12052, https://doi.org/10.1111/ele.12052

McInerney, F. A., & Wing, S. L. (2011). The Paleocene-Eocene Thermal Maximum: A perturbation of carbon cycle, climate, and biosphere with implications for the future. *Annual Review of Earth and Planetary Sciences*, *39*(1), 489–516. Retrieved from https://doi.org/10.1146/annurev-earth-040610-133431

Monteiro, F. M., Bach, L. T., Brownlee, C., Bown, P., Rickaby, R. E. M., Poulton, A. J., & Ridgwell, A. (2016). Why marine phytoplankton calcify. *Science Advances*, *2*(7), e1501822. Retrieved from http://advances.sciencemag.org/content/2/7/e1501822, https://doi.org/10.1126/sciadv.1501822

Monteiro, F. M., Pancost, R. D., Ridgwell, A., & Donnadieu, Y. (2012). Nutrients as the dominant control on the spread of anoxia and euxinia across the Cenomanian-Turonian oceanic anoxic event (OAE2): Model-data comparison. *Paleoceanography*, *27*, PA4209. Retrieved from https://doi.org/10.1029/2012PA002351

Norris, R. (1991). Biased extinction and evolutionary trends. *Paleobiology*, *17*(4), 388–399. https://doi.org/10.1017/S0094837300010721

Norris, R., Kirtland Turner, S., Hull, P., & Ridgwell, A. (2013). Marine ecosystem responses to Cenozoic global change. *Science*, *341*, 492. https://doi.org/10.1126/science.1240543

O'Connor, M. I., Piehler, M. F., Leech, D. M., Anton, A., & Bruno, J. F. (2009). Warming and resource availability shift food web structure and metabolism. *PLOS Biology*, *7*(8), 1–6. Retrieved from https://doi.org/10.1371/journal.pbio.1000178, https://doi.org/10.1371/journal.pbio.1000178

Olonscheck, D., Hofmann, M., Worm, B., & Schellnhuber, H. J. (2013). Decomposing the effects of ocean warming on chlorophyll a concentrations into physically and biologically driven contributions. *Environmental Research Letters*, *8*(1), 14043. Retrieved from http://stacks.iop.org/1748-9326/8/i=1/a=014043

Pörtner, H. O., Karl, D. M., Boyd, P., Chueng, W., Lluch-Cota, S., Nojiri, Y., & Zavialov, P. (2014). Ocean Systems. In C. Field (Ed.), *Climate change 2014: Impacts, adaptation, and vulnerability. Part A: Global and sectoral aspects. Contribution of Working Group II to the Fifth Assessment Report of the Intergovernmental Panel on Climate Change*. Cambridge: Cambridge University Press, pp. 411–484.

Ridgwell, A., Hargreaves, J. C., Edwards, N. R., Annan, J. D., Lenton, T. M., Marsh, R., & Watson, A. (2007). Marine geochemical data assimilation in an efficient Earth system model of global biogeochemical cycling. *Biogeosciences*, *4*(1), 87–104. Retrieved from http://www.biogeosciences.net/4/87/2007/, https://doi.org/10.5194/bg-4-87-2007

Ridgwell, A., & Schmidt, D. N. (2010). Past constraints on the vulnerability of marine calcifiers to massive carbon dioxide release. *Nature Geoscience*, *3*(3), 196–200. https://doi.org/10.1038/ngeo755

Roshan, S., & DeVries, T. (2017). Efficient dissolved organic carbon production and export in the oligotrophic ocean. *Nature Communications*, *8*(1), 2036. https://doi.org/10.1038/s41467-017-02227-3

Schmidt, D. N. (2018). Determining climate change impacts on ecosystems: The role of palaeontology. *Palaeontology*, *61*(1), 1–12. Retrieved from https://doi.org/10.1111/pala.12335

Schmidt, D. N., Lazarus, D., Young, J. R., & Kucera, M. (2006). Biogeography and evolution of body size in marine plankton. *Earth-Science Reviews*, *78*(3), 239–266. Retrieved from http://www.sciencedirect.com/science/article/pii/S0012825206000754, https://doi.org/10.1016/j.earscirev.2006.05.004

Schmidt, D. N., Thierstein, H. R., Bollmann, J., & Schiebel, R. (2004). Abiotic forcing of plankton evolution in the Cenozoic. *Science*, *303*(5655), 207–210. Retrieved From http://science.sciencemag.org/content/303/5655/207, https://doi.org/10.1126/science.1090592

Sluijs, A., Bowen, G., Brinkhuis, H., Lourens, L., & Thomas, E. (2007). The Palaeocene-Eocene Thermal Maximum super greenhouse: Biotic and geochemical signatures, age models and mechanisms of global change. *Geological Society of London, Special Publication Geological*, 323–349.

Ward, B., Dutkiewicz, S., & Follows, M. (2014). Modelling spatial and temporal patterns in size-structured marine plankton communities: Top-down and bottom-up controls. *Journal of Plankton Research*, *36*(1), 31–47. https://doi.org/10.1093/plankt/fbt097

Ward, B., Dutkiewicz, S., Jahn, O., & Follows, M. (2012). A size-structured food-web model for the global ocean. *Limnology and Oceanography*, *57*(6), 1877–1891.

Ward, B. A., & Follows, M. J. (2016). Marine mixotrophy increases trophic transfer efficiency, mean organism size, and vertical carbon flux. *Proceedings of the National Academy of Sciences*, *113*(11), 2958–2963. Retrieved From http://www.pnas.org/content/113/11/2958, https://doi.org/10.1073/pnas.1517118113

Ward, B. A., Wilson, J. D., Death, R. M., Monteiro, F. M., Yool, A., & Ridgwell, A. (2018). EcoGEnIE 1.0: Plankton ecology in the cGEnIE model. *Geoscientific Model Development*, *11*(10), 4241–4267. Retrieved Fromhttps://www.geosci-model-dev.net/11/4241/2018/, https://doi.org/10.5194/gmd-11-4241-2018

Winder, M., & Sommer, U. (2012). Phytoplankton response to a changing climate. *Hydrobiologia*, *698*(1), 5–16. Retrieved From https://doi.org/10.1007/s10750-012-1149-2, https://doi.org/10.1007/s10750-012-1149-2

Young, J. (1990). Size variation of Neogene Reticulofenestra coccoliths from Indian Ocean DSDP cores. *Journal of Micropalaeontology*, *9*(1), 71–85. Retrieved From http://jm.lyellcollection.org/content/9/1/71, https://doi.org/10.1144/jm.9.1.71

Zachos, J. C., Dickens, G. R., & Zeebe, R. E. (2008). An early Cenozoic perspective on greenhouse warming and carbon-cycle dynamics. *Nature*, *451*, 279–283. https://doi.org/10.1038/nature06588